[Journal of Geophysical Research: Atmospheres]

Supporting Information for

Diurnal climatology of planetary boundary layer height over the contiguous United States derived from AMDAR and reanalysis data

Yuanjie Zhang[1], Kang Sun[2], Zhiqiu Gao[1, 3], Zaitao Pan[4], Michael A. Shook[5], Dan Li[6]

[1]School of Atmospheric Physics, Nanjing University of Information Science and Technology, Nanjing 210044, China

[2] Department of Civil, Structural and Environmental Engineering and Research and Education in Energy, Environment and Water Institute, University at Buffalo, Buffalo, NY 14260, USA

[3]State Key Laboratory of Atmospheric Boundary Layer Physics and Atmospheric Chemistry, Institute of Atmospheric Physics, Chinese Academy of Sciences, Beijing 100029, China

[4]Department of Earth and Atmospheric Sciences, Saint Louis University, St. Louis, MO 63103, USA

[5]NASA Langley Research Center, Hampton, VA 23681, USA

[6]Department of Earth and Environment, Boston University, Boston, MA 02215, USA

Corresponding author: Kang Sun (kangsun@buffalo.edu)

Contents of this file

Text S1 to S5
Figures S1 to S16

Introduction

The first part of the supporting information introduces the manual PBLH labelling from DISCOVER-AQ spiral profiles. The second part shows the probability distributions of surface friction velocity from the ERA5 data, comparisons of PBLHs derived from AMDAR data with a constant surface friction velocity to validation data and the frequency of PBL types in each season. The third part shows hourly evolution of PBLH across the CONUS in four seasons. Comparisons between ERA5 PBLHs and AMDAR PBLHs estimated with different parameter sets are shown in the fourth part, and the last part shows seasonally averaged PBLH diurnal variation from AMDAR and ERA5 data over different regions.

Text S1.

To make the PBLH labeling as consistent and accurate as possible, the following rules were observed:

1. The PBLH is determined as the top boundary of a reasonably well-mixed layer that is attached to the surface.

2. The PBLH should collocate with sharp gradients of potential temperature, relative humidity (RH), water vapor, and/or other important tracers (e.g., CO_2, NO_2, aerosol extinction).

3. A lower limit of PBLH is determined as the highest altitude which is fully located in the PBL; an upper limit of PBLH is also determined as the top of the transition zone between the PBL and the layer above (could be the free troposphere, the residual layer, or sometimes other complicated layer structures). The confidence of determination of these two limits is often lower than the PBLH itself.

4. The PBLH is unconfident if either the upper or the lower limit cannot be determined, which is flagged as unidentified and excluded from further analysis.

5. The thickness between the lower and upper limits of PBLH qualitatively characterizes the ambiguity of the manually determined PBLH. When the PBL structure is clear, this thickness represents an estimate of the entrainment zone.

Figure S1 gives an example of a clearly defined PBL during DISCOVER-AQ in Maryland-DC. Profiles of potential temperature, RH, water vapor, CO_2, NO_2, and dry aerosol extinction at 532 nm are normalized to a range of 0 to 1 from the surface to the top of the spiral to facilitate PBLH identification. Figure S2 shows the comparison between PBLHs labeled by Kang Sun and Don Lenschow (Personal communication) for DISCOVER-AQ in Maryland-DC, and Figure S3 shows the comparison between PBLHs labeled by Kang Sun and Michael Shook for DISCOVER-AQ in California. It can be seen that the PBLHs independently labeled by two scientists agree with each other rather well. In the Maryland-DC comparison, there is a group of points where the two versions of manual labelling strongly disagree. These profiles were mostly from July 21, 22, and 28, 2011 when significant cloud coverage was present, and as a result, the PBL was poorly developed in some profiles and challenging to identify. We use the manual PBLHs labelled by Kang Sun in the analysis in Sect. 3.3 considering their consistency and completeness of all DISCOVER-AQ phases.

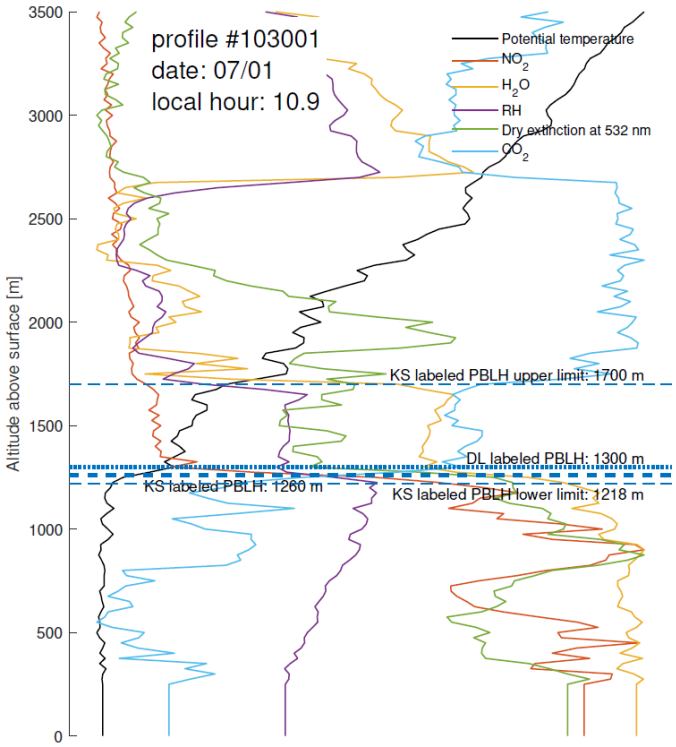

63
64

65 **Figure S1.** The determination of PBLH based on DISCOVER-AQ profiles. The potential
66 temperature and tracer profiles are scale from 0 to 1 to facilitate gradient identification. KS:
67 PBLH labeled by Kang Sun; DL: PBLH independently labeled by Don Lenschow.

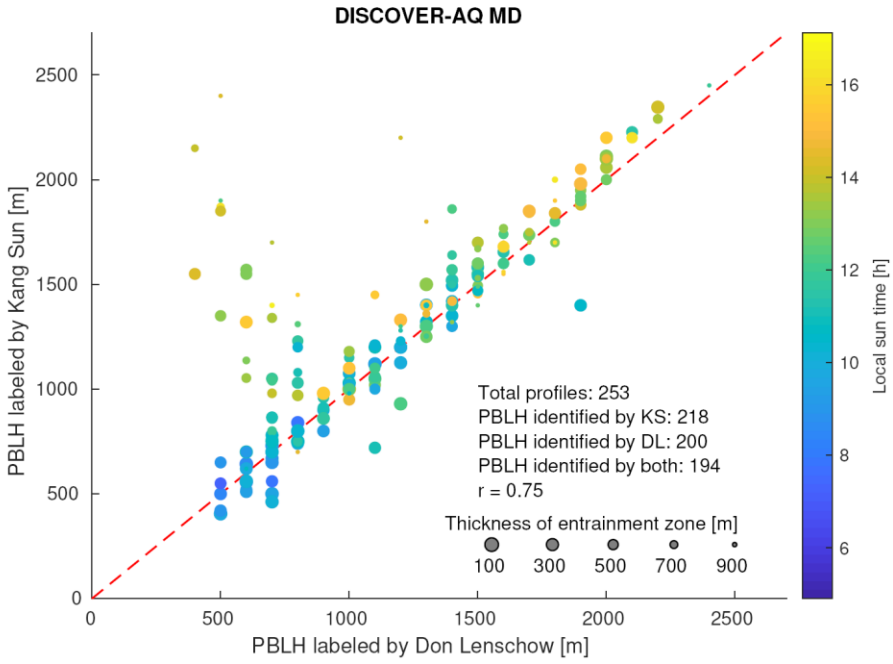

68

69 **Figure S2.** Comparison between PBLH labeled by Kang Sun and Don Lenschow for
70 DISCOVER-AQ MD. The red dashed line is 1:1.

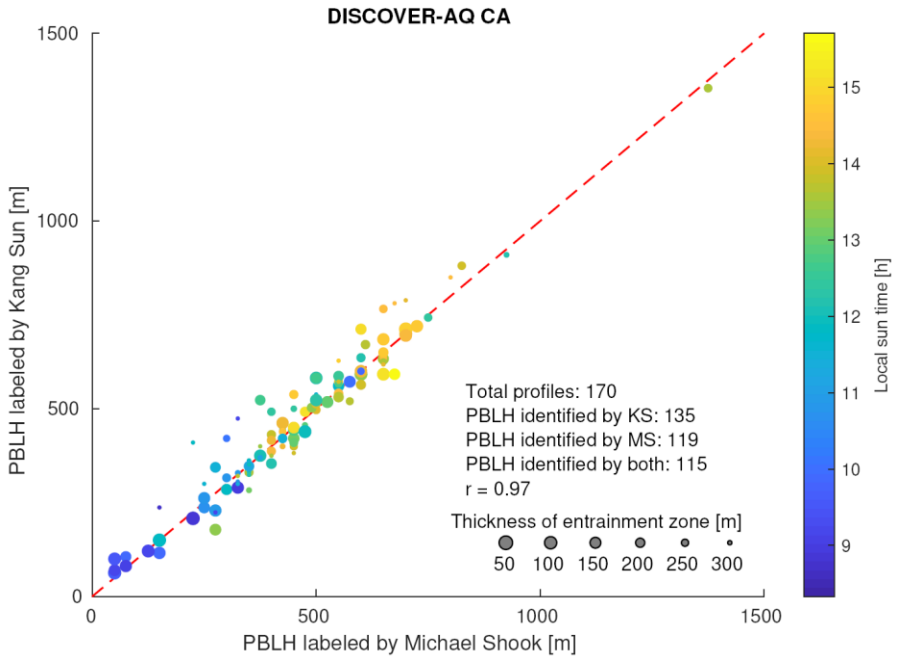

Figure S3. Comparison between PBLH labeled by Kang Sun and Michael Shook for DISCOVER-AQ CA. The red dashed line is 1:1.

Text S2.

The ERA5 surface friction velocity (u_*) sampled at AMDAR observation time and the nearest grid cells to the AMDAR airports increases with decreasing stratification stability, with a median value as 0.16, 0.20 and 0.22 for stable boundary layers (SBLs), near-neutral boundary layers (NBLs) and convective boundary layers (CBLs) (Figure S4). With a larger constant u_* of 0.3 m/s relative to ERA5 u_*, the AMDAR PBLHs estimated by the parameter set of $Ri_{bc} = 0.5$, $b = 100$ and $z_s = 40$ m show better agreements with validation data at CO and MD, with correlation coefficients as 0.65 and 0.57, respectively, while slightly worse agreements at TX and ARM-SGP, compared to results in Figure 4 (Figure S5). The frequency of daytime PBL types varies by season. As can be seen, daytime SBLs are more prevalent in autumn and winter (Figure S6).

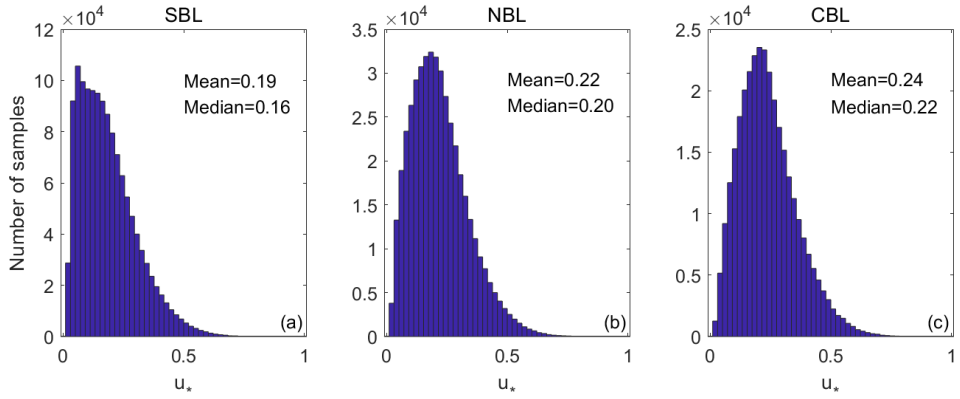

Figure S4. The probability distributions of surface friction velocity (u_*) from the ERA5 data for (a) SBL, (b) NBL and (c) CBL at the nearest grids to the 54 AMDAR airports and at hours when there is an AMDAR profile during 2007-2016.

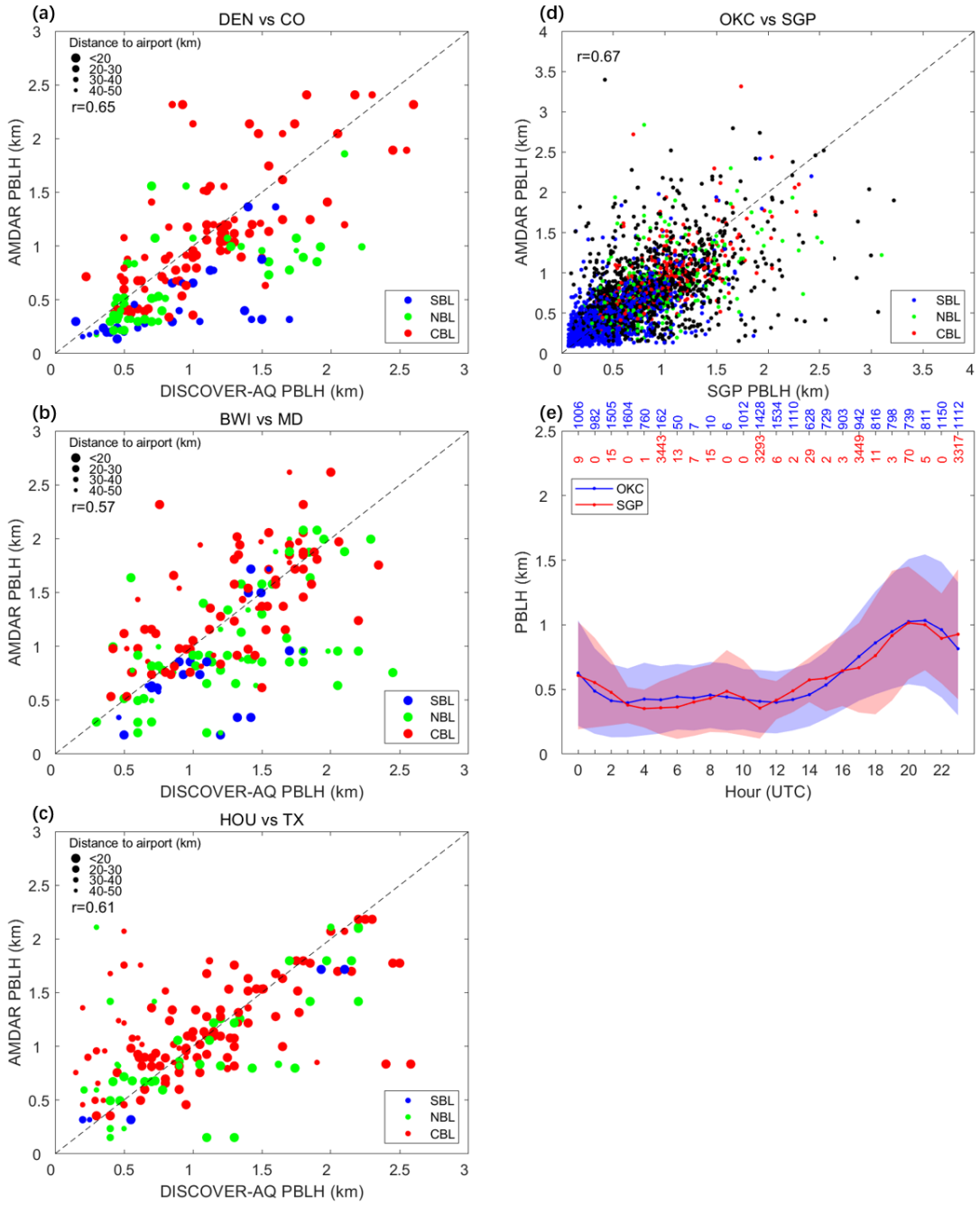

Figure S5. Comparisons of PBLHs derived from AMDAR data with the parameter set Ri_{bc}=0.5, u_* =0.3 m/s (b = 100), z_s=40 m to PBLHs from DISCOVER-AQ data at (a) CO, (b) MD, (c) TX, and from (d-e) ARM-SGP data.

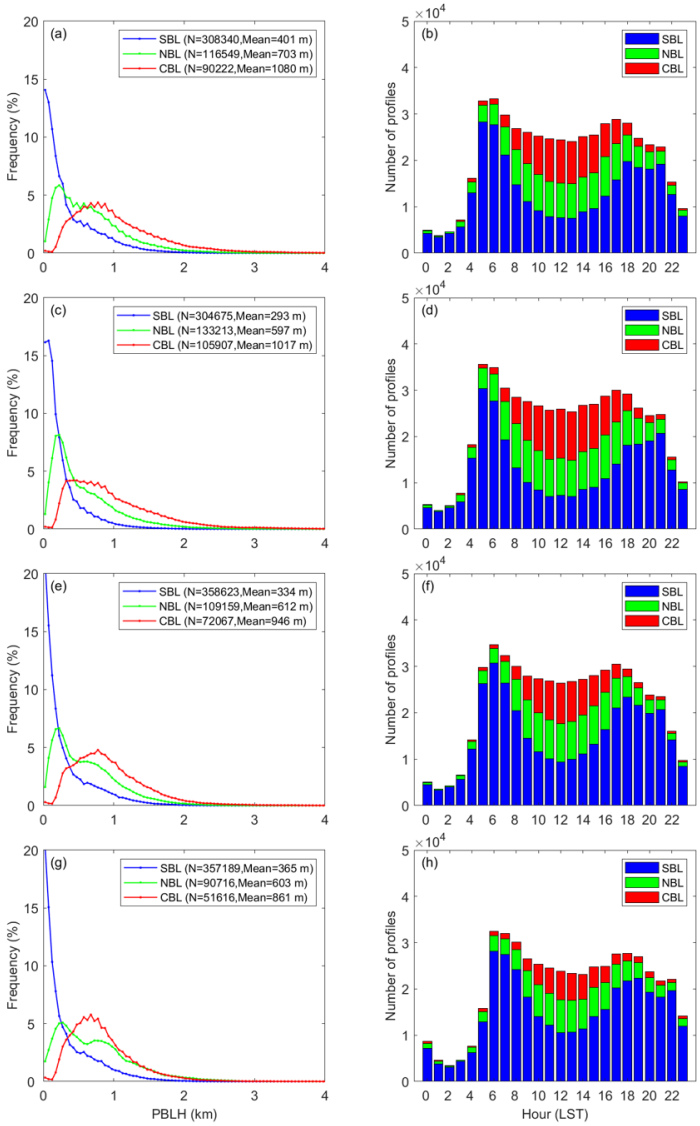

Figure S6. Similar to Figure 5, but in (a-b) spring, (c-d) summer, (e-f) autumn and (g-h) winter.

Text S3.

Hourly evolution of PBLH across the CONUS in four seasons are shown in Figure S7-S10.

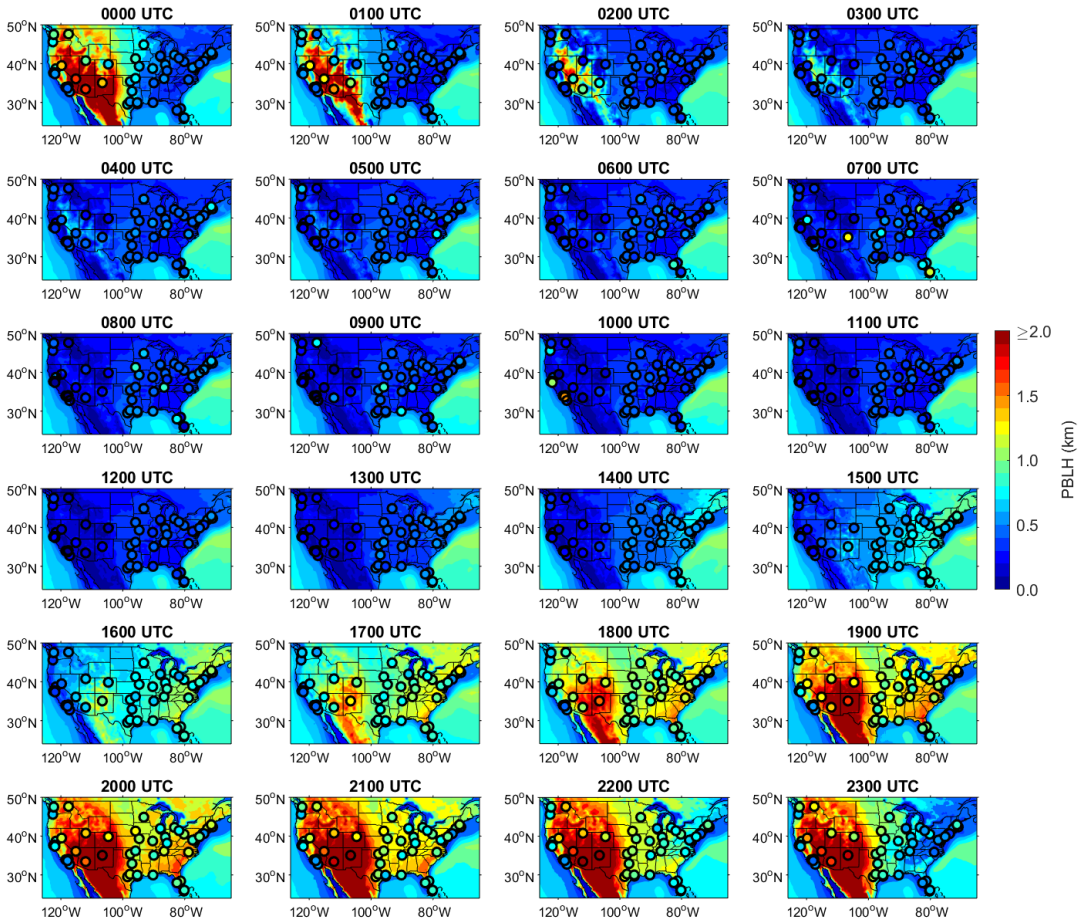

Figure S7. Spatial distribution of mean PBLH at each UTC hour in spring from the AMDAR profiles (dot symbols) and from ERA5 data (background color).

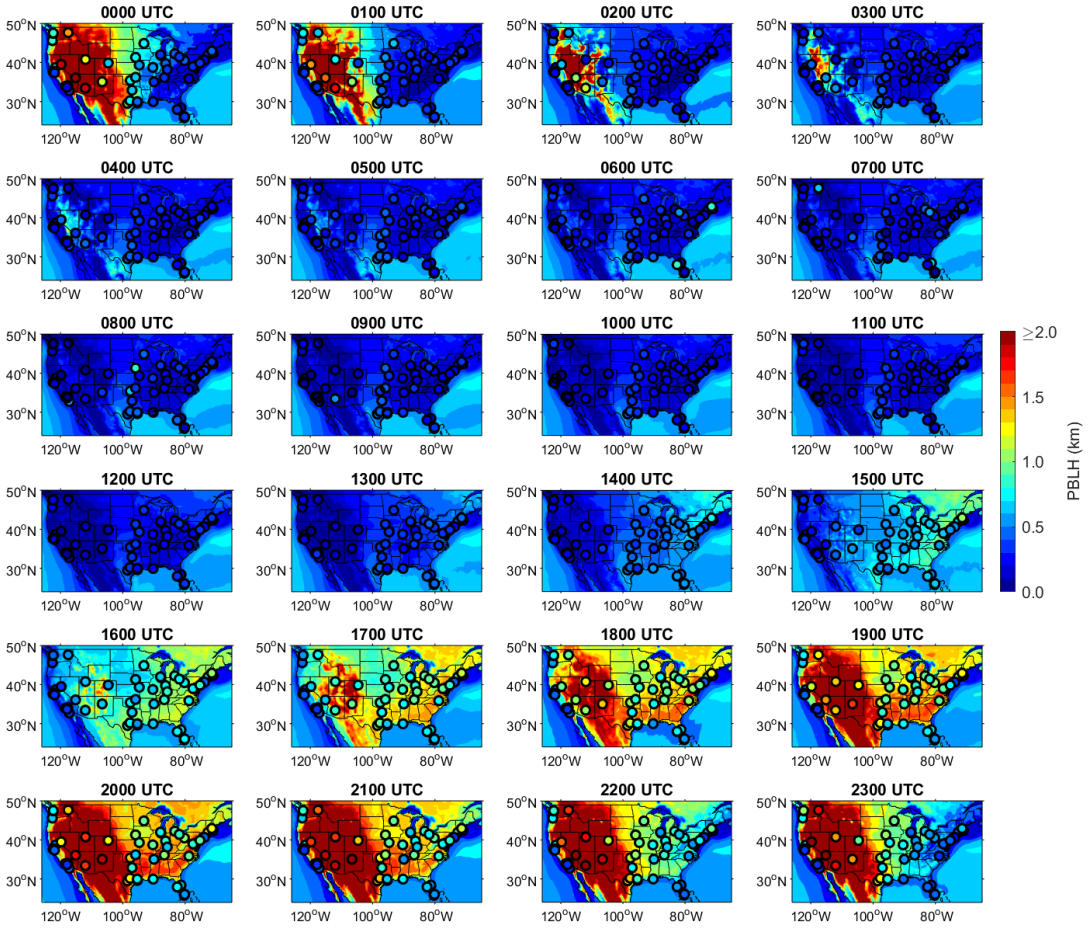

106

107 **Figure S8.** Similar to Figure S7, but in summer.

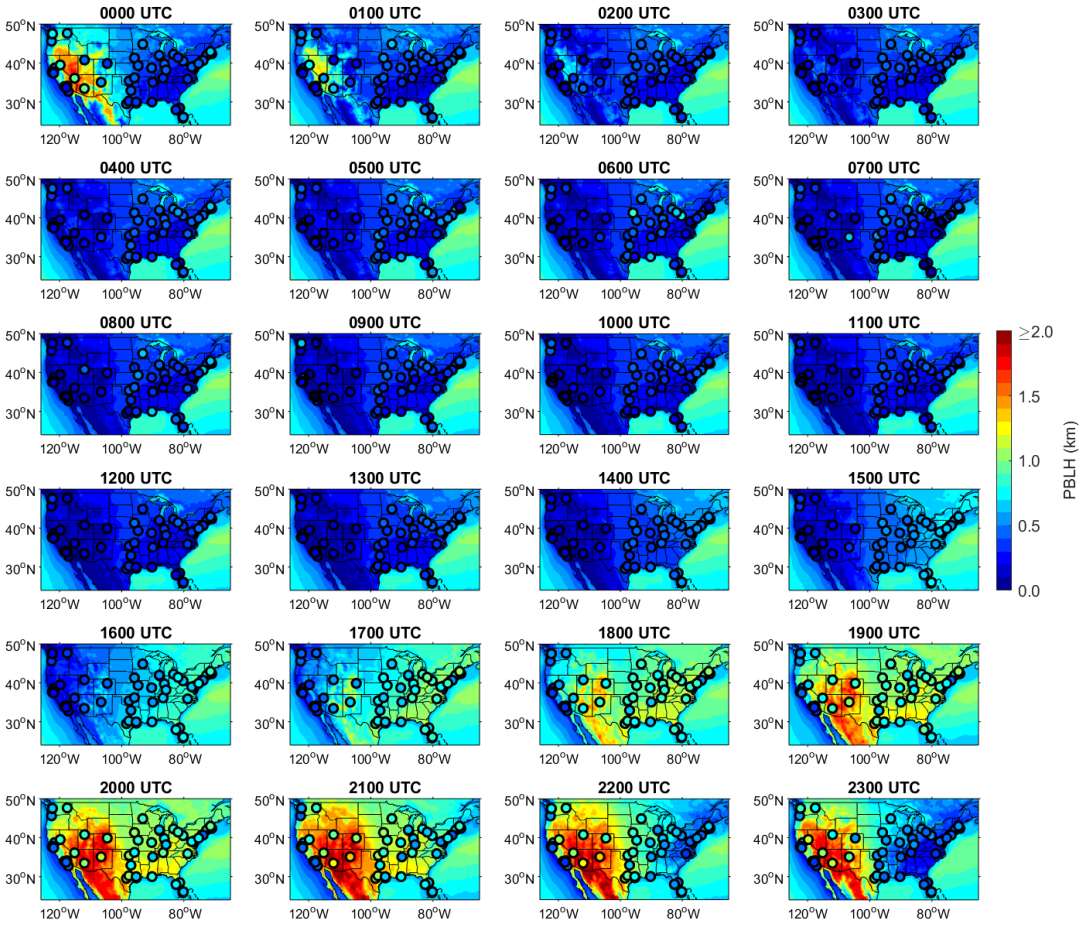

108

109 **Figure S9.** Similar to Figure S7, but in autumn.

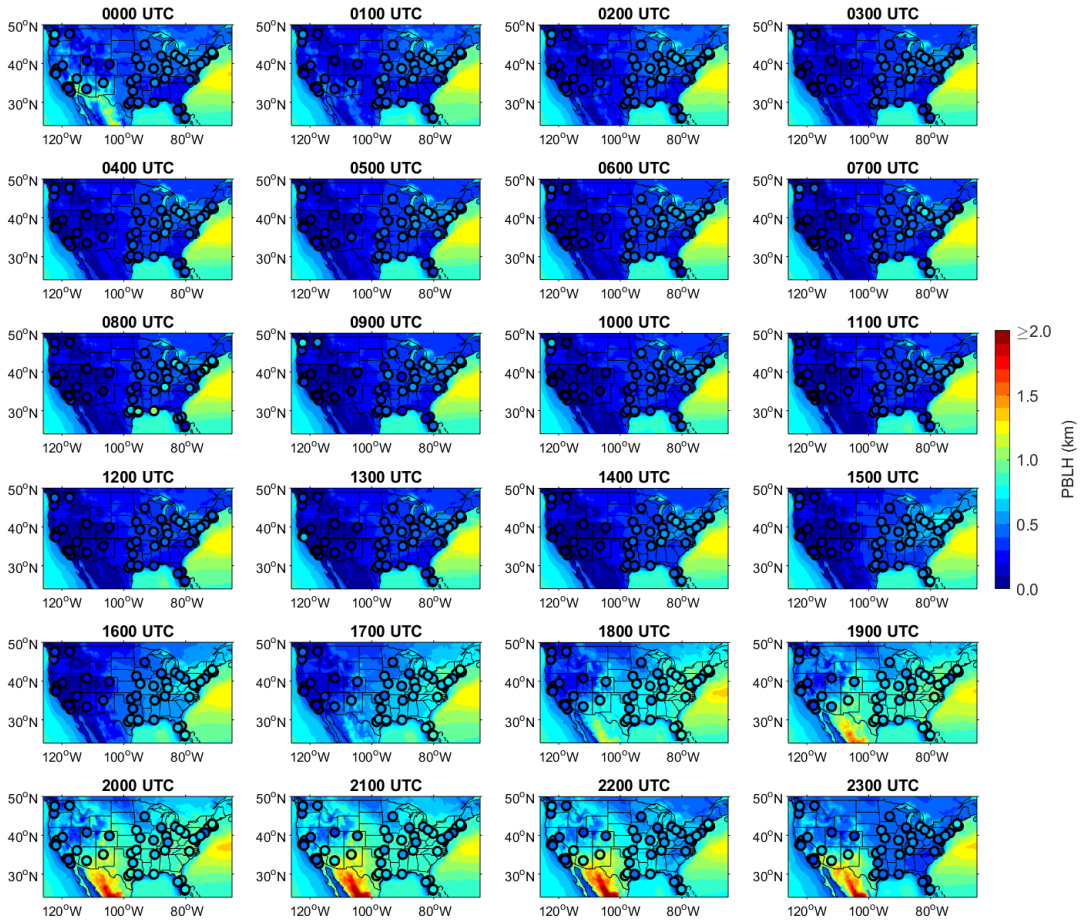

110

111 **Figure S10.** Similar to Figure S7, but in winter.

Text S4.

Comparisons between ERA5 PBLHs and AMDAR PBLHs estimated with the same parameters (Ri_{bc} = 0.25, b = 0) are shown in Figure S11. The results show even larger biases during daytime and opposite biases at nighttime compared to those in Figure 11. Comparisons are also conducted between ERA5 PBLHs and AMDAR PBLHs estimated with the parameter set of Ri_{bc} = 0.5, u_* =0.3 m/s (b = 100) and z_s = 40 m, as shown in Figure S12. One can see larger nighttime biases due to the overall higher AMDAR PBLHs across the diurnal cycles compared to results in Figure 11.

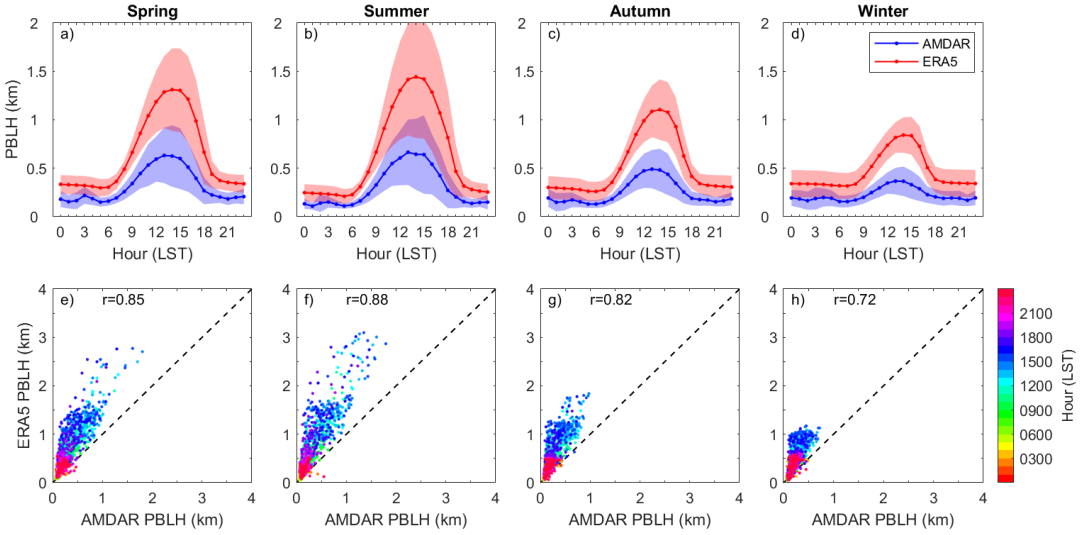

Figure S11. Similar to Figure 11, but the PBLHs from AMDAR data are estimated using the parameter set of Ri_{bc} = 0.25, b = 0 and z_s = 40 m.

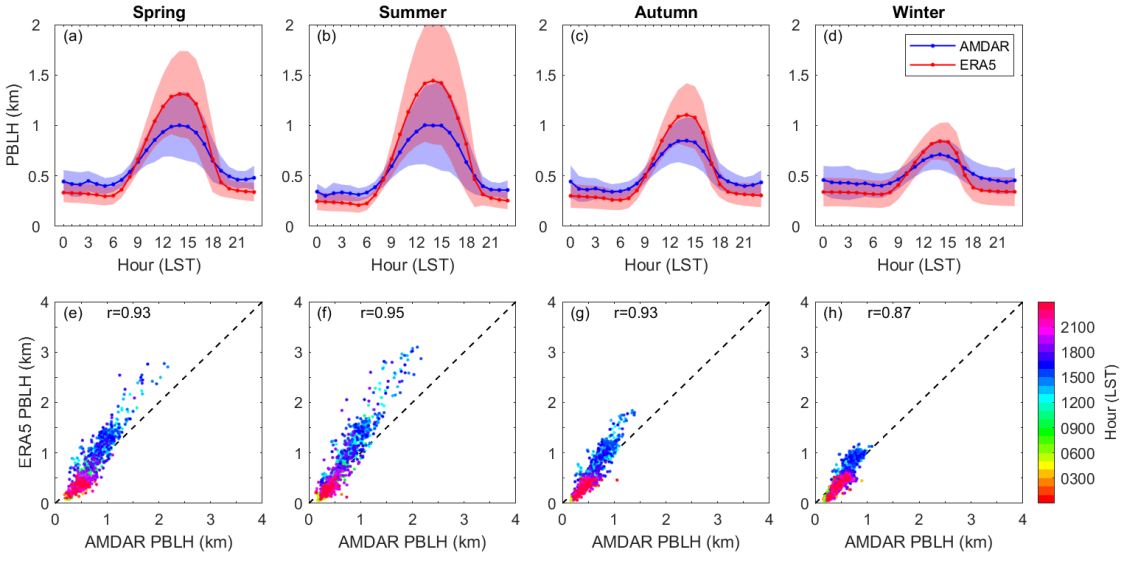

Figure S12. Similar to Figure 11, but the PBLHs from AMDAR data are estimated using the parameter set of Ri_{bc} = 0.5, u_* =0.3 m/s (b = 100) and z_s = 40 m.

Text S5.

Seasonally averaged PBLH diurnal variation from AMDAR and ERA5 data over different regions are shown in Figure S13-S16.

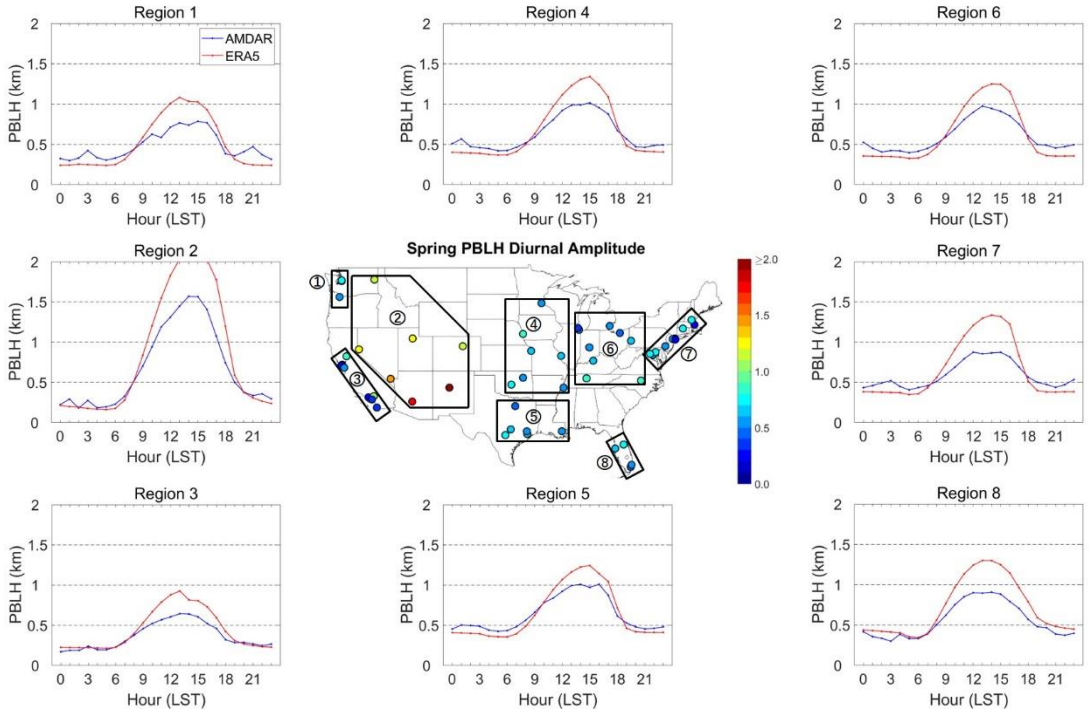

Figure S13. Diurnal amplitude (maximum minus minimum, unit is km) of PBLH based on AMDAR data at 54 airports (center), and the spatially averaged diurnal cycles of PBLH over 8 regions. The results are spring averages over the period 2007-2016.

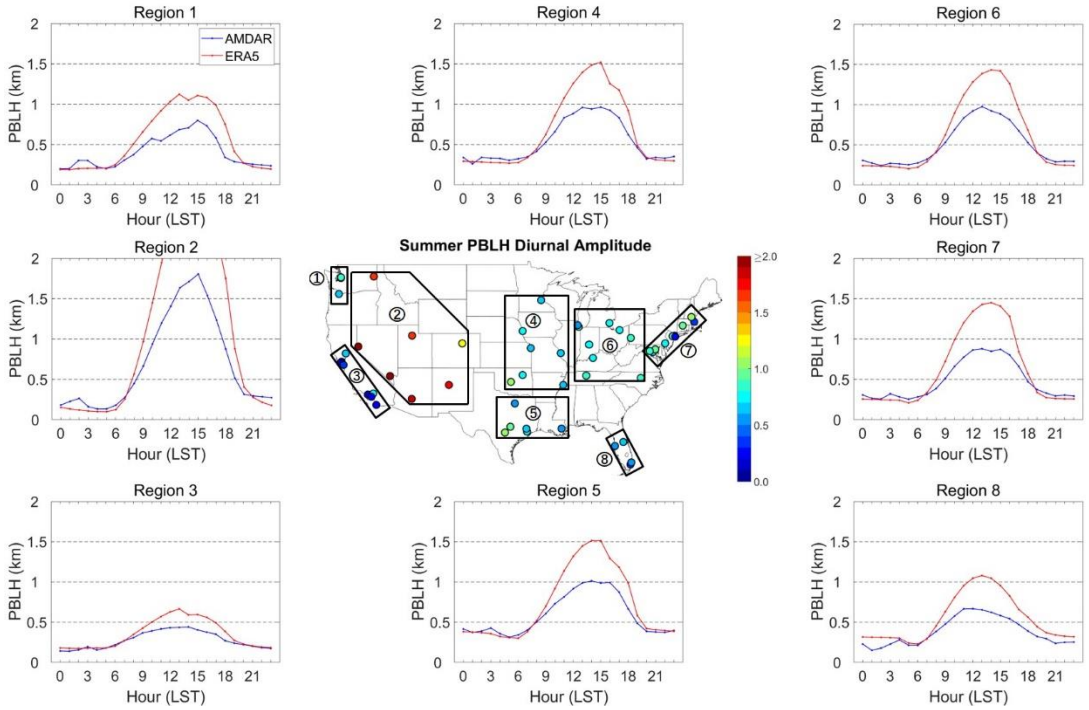

Figure S14. Similar to Figure S13, but for summer averages.

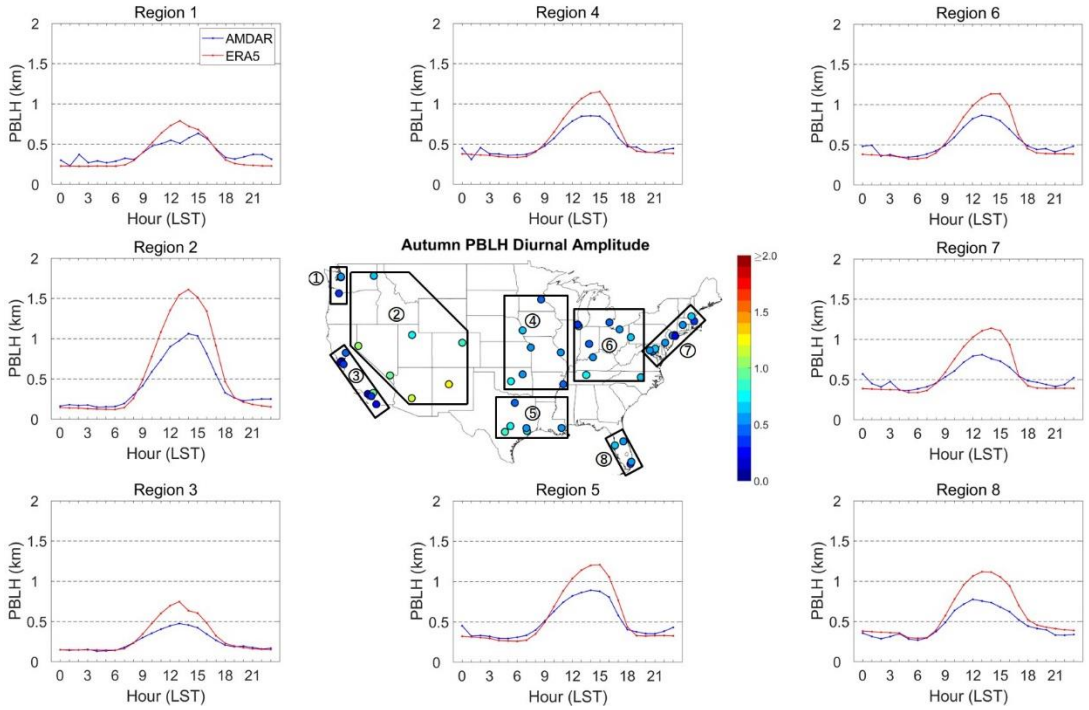

Figure S15. Similar to Figure S13, but for autumn averages.

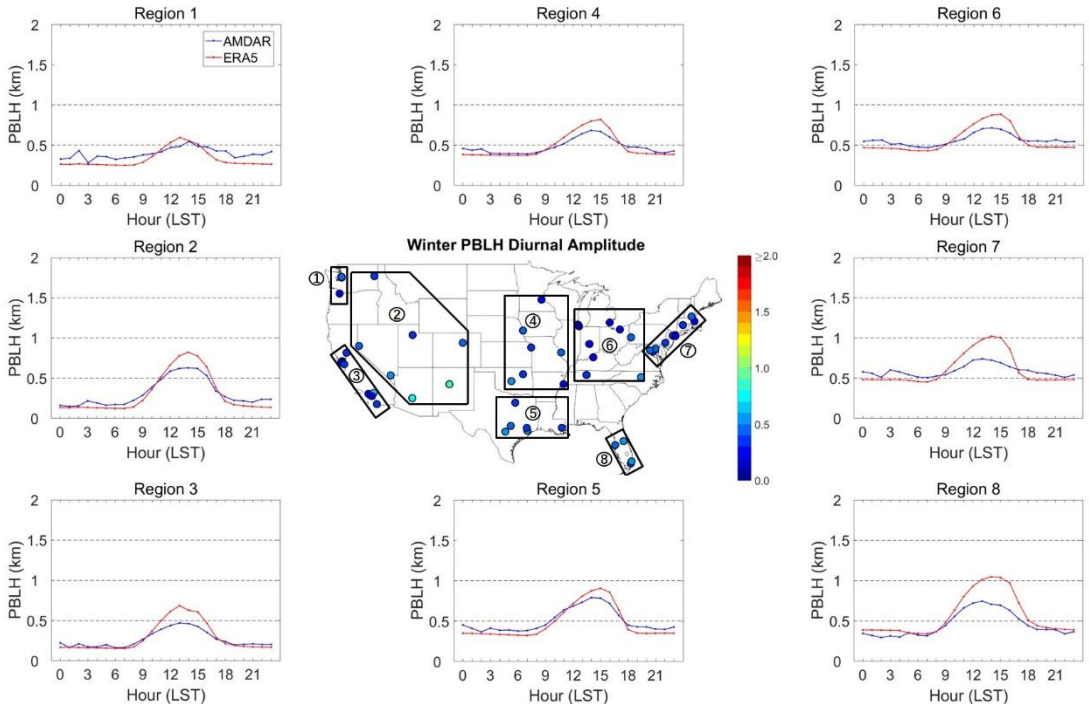

141

142 **Figure S16.** Similar to Figure S13, but for winter averages.